Role of the S4-S5 Linker in CNG Channel Activation

Jana Kusch,[†△] Thomas Zimmer,[†△] Jascha Holschuh,[†] Christoph Biskup,[†‡] Eckhard Schulz,[§] Vasilica Nache,[†] and Klaus Benndorf[†*]

[†]Universitätsklinikum Jena, Institut für Physiologie II, Jena, Germany; [‡]Universitätsklinikum Jena, Arbeitsgruppe für Biomolekulare Photonik, Jena, Germany; and [§]Fachhochschule Schmalkalden, Fakultät Elektrotechnik, Schmalkalden, Germany

ABSTRACT Cyclic nucleotide-gated (CNG) channels mediate sensory signal transduction in retinal and olfactory cells. The channels are activated by the binding of cyclic nucleotides to a cyclic nucleotide-binding domain (CNBD) in the C-terminus that is located at the intracellular side. The molecular events translating the ligand binding to the pore opening are still unknown. We investigated the role of the S4-S5 linker in the activation process by quantifying its interaction with other intracellular regions. To this end, we constructed chimeric channels in which the N-terminus, the S4-S5 linker, the C-linker, and the CNBD of the retinal CNGA1 subunit were systematically replaced by the respective regions of the olfactory CNGA2 subunit. Macroscopic concentration-response relations were analyzed, yielding the apparent affinity to cGMP and the Hill coefficient. The degree of functional coupling of intracellular regions in the activation gating was determined by thermodynamic double-mutant cycle analysis. We observed that all four intracellular regions, including the relatively short S4-S5 linker, are involved in controlling the apparent affinity of the channel to cGMP and, moreover, in determining the degree of cooperativity between the subunits, as derived from the Hill coefficient. The interaction energies reveal an interaction of the S4-S5 linker with both the N-terminus and the C-linker, but no interaction with the CNBD.

INTRODUCTION

Cyclic nucleotide-gated (CNG) channels are nonselective cation channels expressed in various neuronal and non-neuronal cell types (1–3). They are best characterized in rod photoreceptors and olfactory neurons, generating the light- and odor-induced electrical response, respectively (3,4). Native CNG channels are tetrameric proteins which are composed in the photoreceptors of two (CNGA1, CNGB1) and in the olfactory neurons of three (CNGA2, CNGA4, CNGB1b) homolog subunits (5–10). Only one type of subunit of each native channel (CNGA1, CNGA2) forms functional channels on its own when expressed in heterologous cells. Each subunit is composed of six transmembrane segments with a pore loop between segment S5 and S6. The intracellular C-terminal part carries a cyclic nucleotide-binding domain (CNBD) that is connected to the S6 domain by the C-linker. Together with these regions, the N-terminus and the S4-S5 linker are located at the intracellular side.

Functionally, the binding of cyclic nucleotides to the intracellular binding domains strongly promotes the opening of the channel (11). Various experimental results suggest that the conformational change of the CNBD induced by the ligand binding is transferred to the channel pore via the C-linker (12–16). The conformational changes in the C-linker are supposed to cause conformational changes in the S6 segment which leads finally to an opening of the activation gate inside the pore. It is therefore not surprising that not only the CNBD but also the C-linker determines the sensitivity of CNG channels to cyclic nucleotides (12–15,17,18). In addition to this, the N-terminus has been identified as a determinant for this sensitivity (12,19,20). Further structural and functional data suggest interactions between the C-linker and the N-terminus (18,21,22), the C-linker and the CNBD, and the C-linkers of neighbored subunits (22–25).

While there is no doubt about an involvement of the CNBD, the C-linker, and the N-terminus in the activation gating of CNG channels, little is known about the role of the S4-S5 linker. In CNG channels, this region is a short loop of only 11 amino acids, differing between CNGA1 and CNGA2 in only one amino acid (11,26). Most likely, it does not form a helical structure. This is in contrast to related voltage-gated potassium channels and HCN channels, where the S4-S5 linker forms an α-helical structure and thus a rigid connection between the voltage sensor domain and the pore lining domain S5 (27–29). It has been proposed that the absence of a helical structure in CNG channels is the cause for the functional uncoupling of the voltage sensor domain from the pore-forming domain, leaving only a minor voltage dependence (30). It has been reported that the S4-S5 linker in CNG channels plays a role in the blocking mechanism of the state-dependent blocker dequalinium (31).

For the activation of CNG channels, Hill coefficients > 1 have been determined, ranging from 1.5 to 3.5. This directly indicates that more than one subunit is involved in the activation gating (3). In CNGA2 channels, we previously showed that the cooperativity of binding is both positive and negative (32,33). Being aware that the Hill coefficient

Submitted February 28, 2010, and accepted for publication July 19, 2010.

△J. Kusch and T. Zimmer contributed equally to this work.

*Correspondence: klaus.benndorf@mti.uni-jena.de

Editor: Michael Pusch.

0006-3495/10/10/2488/9 $2.00

doi: 10.1016/j.bpj.2010.07.041

does not only depend on the ligand binding but also on the subsequent processes (34,35), any Hill coefficient determined from electrophysiological measurements can only be a lower estimate for the number of ligands involved in the activation gating, and does not specify the true number. Nevertheless, a changed Hill coefficient, e.g., by mutating a channel, can be taken as a change in the total degree of cooperativity during the activation process (36).

Herein, we investigated the role of the S4-S5 linker for CNG channel activation and, in particular, its interaction with the other intracellular regions N-terminus, C-linker, and CNBD. For this purpose, chimeras were constructed with either one, two, three, or all four CNGA2 regions in a CNGA1 background. We show that all four regions, including the S4-S5 linker, are involved in determining the apparent affinity of the channel to cGMP and that they contribute differently to the cooperativity of the subunits in the activation process. Interaction energies between the intracellular regions were quantified according to the principle of double-mutant cycle analysis.

MATERIALS AND METHODS

Construction of chimeric CNGA1/CNGA2 channels

The α-subunits of bovine rod (CNGA1) and olfactory channels (CNGA2) (accession No. X51604 and X55010, respectively), as well as chimeras oN, oCL, oB, oNB, and oCLB were kindly provided by U. B. Kaupp (Caesar Bonn, Germany). Chimeras o45, o45CL, o45B, and o45CLB were constructed by polymerase-chain-reaction-mediated insertion of serine 268 of CNGA2 at the corresponding alignment position in CNGA1, oCL, oB, and oCLB, respectively. All other chimeras were obtained by using suitable precursor constructs as templates and common restriction sites, as follows:

- *Sna*BI/*Xho*I sites were used to construct oNCLB from templates oN and oCLB.
- *Sna*BI/*Nsi*I sites were used for the construction of oN45 from oN and o45, and of oN45CLB from oNCLB and o45CLB.
- *Sna*BI/*Sal*I sites were used for the construction of oNCL from oN and oCL, of oN45B from oN and o45B, and of oN45CL from oN45 and o45CL.

Table 1 illustrates names and structures of all chimeras used in this study. The names are related to the sequence of the transferred CNGA2 regions into a CNGA1 background (*N* = N-terminus, *45* = S4-S5 linker, *CL* = C-linker, *B* = cyclic nucleotide-binding domain). An "o" before a region indicates that an "olf" (CNGA2) region was transferred.

TABLE 1 Structure of the CNGA1/CNGA2 chimeras

Chimera	Structure
CNGA1 (rod)	rM1-D690
oN	oM1-D134 rP158-D690
o45	rM1-T290 oS268 rY292-D690
oCL	rM1-I390 oV368-P477 rG501-D690
oB	rM1-P500 oG478-P663
oN45	oM1-D134 rP158-T290 oS268 rY292-D690
oNCL	oM1-D134 rP158-I390 oV368-P477 rG501-D690
oNB	oM1-D134 rP158-P500 oG478-P663
o45CL	rM1-T290 oS268 rY292-I390 oV368-P477 rG501-D690
o45B	rM1-T290 oS268 rY292-P500 oG478-P663
oCLB	rM1-I390 oV368-P663
oN45CL	oM1-D134 rP158-T290 oS268 rY292-I390 oV368-P477 rG501-D690
oN45B	oM1-D134 rP158-T290 oS268 rY292-P500 oG478-P663
oNCLB	oM1-D134 rP158-I390 oV368-P663
o45CLB	rM1-T290 oS268 rY292-I390 oV368-P663
oN45CLB	oM1-D134 rP158-T290 oS268 rY292-I390 oV368-P663
CNGA2 (olf)	oM1-P663

Oocyte preparation and cRNA injection

Ovarian lobes from *Xenopus laevis* were obtained under anesthesia (0.3% 3-aminobenzoic acid ethyl ester) and transferred to a petri dish containing oocyte ringer (OR2): 82.5 mM NaCl, 2 mM KCl, 1 mM $MgCl_2$, 5 mM HEPES, pH 7.5 (NaOH). Oocytes in stages V and VI were prepared by incubation for 20–30 min in OR2 containing either 1 or 2 mg/mL collagenase (Roche, Germany). Within 2–7 h after isolation and defolliculation, cRNA specific for the respective channel/chimera was injected into the oocytes through glass micropipettes. Oocytes were further incubated in Barth medium containing: 84 mM NaCl, 1 mM KCl, 2.4 mM $NaHCO_3$, 0.82 mM $MgSO_4$, 0.33 mM $Ca(NO_3)_2$, 0.41 mM $CaCl_2$, 7.5 mM TRIS, pH 7.4 (HCl), at 18°C for 2–7 days until experimental use. Before patching, the vitelline membrane of the oocytes was mechanically removed.

Electrophysiology

The experiments were performed on the stage of an inverted microscope with standard techniques. The patch pipettes were pulled from quartz glass tubing (Biomedical Instruments, Jena, Germany) with an outer diameter of 1.0 mm and an inner diameter of 0.7 mm. The resistance of the pipette was 0.7–2.0 MΩ. The bath and the pipette solution contained 150 mM KCl, 1 mM EGTA, and 5 mM HEPES, pH 7.4 (KOH). Currents were recorded in inside-out multichannel patches (37). The channels were activated by replacing the bath solution with a respective solution containing cGMP. Each excised patch was first exposed to a saturating cGMP concentration to determine the maximum current. To test for rundown, at a second time, a saturating concentration of cGMP at the end of each measurement was applied. Recordings showing rundown were excluded.

Currents were recorded with an Axopatch 200B amplifier (Molecular Devices, Sunnyvale, CA) controlled by the patch-clamp software ISO2 (MFK, Niedernhausen, Germany) on a PC. The currents were filtered at a cutoff frequency of 10 kHz. The holding voltage was 0 mV. The membrane voltage was first stepped to −100 mV and then to +100 mV. The pulse duration and the repetition rate of the pulses were chosen such that at the end of a pulse the current amplitude was constant (Fig. 1). All measurements were performed at room temperature (22–24°C). The currents were finally corrected for the capacitive and the very small leak components by subtracting respective currents in the absence of cGMP in the bath solution. The currents considered herein are averages of 5–15 consecutive recordings.

Concentration-response relations were determined from the steady-state current at +100 mV by normalizing the current I at the actual cGMP concentration with respect to the current I_{max} at a saturating cGMP concentration. By fitting the data points with the Hill equation

$$\frac{I}{I_{max}} = \frac{1}{1 + \left(\frac{EC_{50}}{[cGMP]}\right)^{H}}, \quad (1)$$

the values for EC_{50} (cGMP concentration of half-maximum activity of the channels) and H (Hill coefficient) were obtained. The curves were fitted to the data with a nonlinear approximation algorithm.

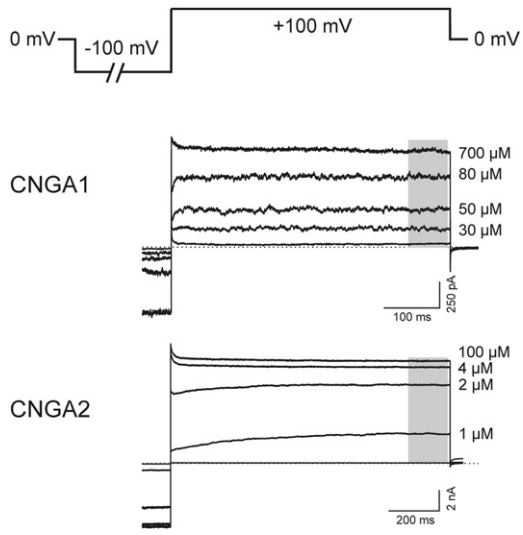

FIGURE 1 Method used to obtain concentration-response relationships in multichannel inside-out patches. The pulse protocol, in which the pulse duration and the repetition rate of the pulses were chosen such that at the end of a pulse the current amplitude was constant, is illustrated. The shade of gray in the representative currents from the two wild-type channels, CNGA1 and CNGA2, indicates the part of the trace that accounted for the determination of the current amplitude.

Double-mutant cycle analysis

The overall reaction of channel opening can be represented by Scheme 1:

$$\mathrm{C} + n\,\mathrm{cGMP} \rightarrow \mathrm{O} \qquad \text{(Scheme 1)}$$

where C is the closed state, O the open state, and n the number of ligands bound.

The Gibbs free energy, $\Delta_r G$, of the channel opening reaction is defined as the difference in the Gibbs free energies of the liganded open (μ_O) and the unliganded closed state (μ_C) and of the solvated ligand (μ_{cGMP}):

$$\Delta_r G = \mu_O - \mu_C - n\mu_{cGMP}. \qquad (2)$$

By taking into account the concentration dependence of the chemical potentials, Eq. 2 can be transformed to

$$\Delta_r G = \Delta_r G^{\oplus} + RT\ln K, \qquad (3a)$$

$$K = \frac{[O]}{[C][cGMP]^n}, \qquad (3b)$$

where R is the molar gas constant, T the temperature in Kelvin, and K the equilibrium constant of the channel opening reaction. Here, $[C]$ is the fraction of closed channels, $[O]$ is the fraction of open channels, and $[cGMP]$ is the ligand concentration. $\Delta_r G^{\oplus}$ is the difference of the molar Gibbs free energies in the biological standard state. At equilibrium, $\Delta_r G$ is zero. Thus, the difference of the standard molar Gibbs free energies is given by

$$\Delta_r G^{\oplus} = \mu_O^{\oplus} - \mu_C^{\oplus} - n\mu_{cGMP}^{\oplus} = -RT\ln K. \qquad (4)$$

By definition, at the EC_{50} the fraction of open and closed states is 0.5 ([O] = [C] = 0.5). If it is assumed that the number of ligands effectively contributing to the activation process is given by the Hill coefficient, H, the equilibrium constant K (Eq. 3 *b*) becomes

$$K = \frac{1}{[EC_{50}]^H}, \qquad (5)$$

yielding

$$\Delta_r G^{\oplus} = HRT\ln[EC_{50}]. \qquad (6)$$

Hence, $\Delta_r G^{\oplus}$ can be calculated from EC_{50} and H.

In principle, substitution of a channel region can modify both the closed and the open state. If a substituted region causes an increase in $\Delta_r G^{\oplus}$, this can be the result of a stabilization of the closed state, a destabilization of the open state, or a combination of both effects. Vice versa, a decrease in $\Delta_r G^{\oplus}$ indicates that the closed state is destabilized and/or that the open state is stabilized by the substitution.

To decide whether the effects of two intracellular regions on channel gating are coupled, interaction energies $\Delta_{int} G^{\oplus}$ can be calculated according to the principles of thermodynamic double-mutant cycle analysis (for review, see 38–40).

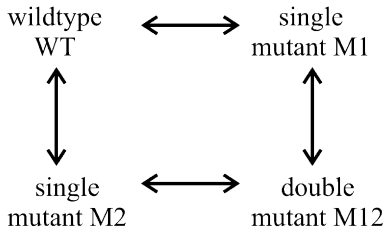

(Scheme 2a)

A double-mutant cycle consists of a wild-type protein, two single mutants, and the corresponding double-mutant (Scheme 2 *a*). In this study, a substituted intracellular CNG channel region was treated like a mutation (compare to (41)).

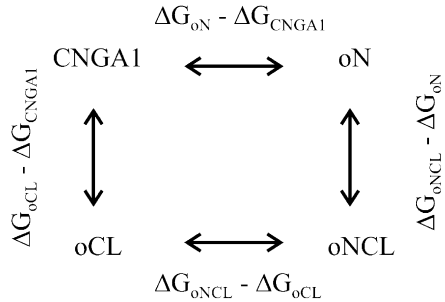

(Scheme 2b)

Scheme 2 *b* illustrates an example of a double-mutant cycle for CNG channel chimeras with N-terminus and/or C-linker substituted.

The interaction energy, $\Delta_{int} G^{\oplus}$, can be determined by comparing the effect of substituting region 1 in the wild-type and the effect of introducing the same substitution in a channel where already a second region was substituted (see Scheme 2, *a* and *b*):

$$\Delta_{int} G^{\oplus} = \left(\Delta_r G^{\oplus}_{M12} - \Delta_r G^{\oplus}_{M2}\right) - \left(\Delta_r G^{\oplus}_{M1} - \Delta_r G^{\oplus}_{wt}\right). \qquad (7)$$

If two noninteracting regions are substituted, then their effects on $\Delta_{int} G^{\oplus}$ of the channel gating reaction are additive. In this case, the interaction energy $\Delta_{int} G^{\oplus}$ is zero. If, however, the substituted domains interact with each other, their interaction energy differs from zero. $\Delta_{int} G^{\oplus}$refers to the difference of the interaction energy between the CNGA1 and CNGA2 channel. $\Delta_{int} G^{\oplus}$does not indicate the interaction energy per se.

The above considerations hold also for a mutant cycle consisting of a triple chimera, two double chimeras, and a single chimera, whose

substitution is also present in both double chimeras and the triple chimera, and, furthermore, for a mutant cycle with a quadruple chimera, two triple chimeras, and a double chimera.

Statistics

Statistical data are given as mean ± SE. A *t*-test with a significance level $p < 0.05$ was used to detect differences between EC_{50} values or Hill coefficients. SE of $\Delta_{int}G^{\oplus}$ was calculated according to the error propagation law.

RESULTS

Effect of the intracellular S4-S5 linker on the apparent affinity for cGMP

The EC_{50} values for homotetrameric CNGA1 and CNGA2 channels to bind cGMP differ significantly (55.9 ± 2.4 μM in CNGA1, 1.39 ± 0.06 μM in CNGA2), indicating different apparent affinities for the ligand. As shown previously, substitution of different regions in CNGA1 by the corresponding regions of CNGA2, and vice versa, led to a partial transfer of the EC_{50} value from the donor to the acceptor channel (12,20). Among these regions are the C-linker and the N-terminus. Paradoxically, the CNBD produced an opposite effect: The low EC_{50} value of the CNGA2 channel is further decreased when transferring the CNGA1 CNBD to CNGA2 and the high EC_{50} value of the CNGA1 channel is further increased when transferring the CNGA2 CNBD to CNGA1 (Fig. 2) (20).

When transferring the CNGA2 S4-S5 linker, another intracellular region, into a CNGA1 background, the EC_{50} value was also significantly decreased (33.5 ± 1.3 μM in chimera o45 versus 55.9 ± 2.4 μM in CNGA1; see Fig. 2). To study this effect with respect to the nature of the other intracellular regions N-terminus, C-linker, and CNBD, we determined the EC_{50} value in CNGA1 chimeras in which a second, third, and fourth region besides the S4-S5 linker were substituted by the respective region of CNGA2 (Fig. 2). The results are:

1. With a second CNGA2 region replaced, the N-terminus did not abolish the S4-S5 linker effect, the C-linker inverted it, and the CNBD neutralized it.
2. In the presence of CNGA2 N-terminus plus C-linker there was no further effect of the S4-S5 linker, possibly due to the opposite effects of the two additional regions.
3. The modulatory effect of the CNGA2 C-linker, but not of the N-terminus, could be neutralized by the CNBD effect.

Effect of the intracellular S4-S5 linker on the Hill coefficient

Notably, substitution of the S4-S5 linker in CNGA1 by the respective region of CNGA2 did not only change the apparent affinity of the resulting chimera, but also decreased the Hill coefficient, *H* (Fig. 3 *A*). Because it is generally possible to relate the Hill coefficient of a concentration-response relation to the extent of cooperativity among the binding sites (subunits) (36), the observed decrease of *H* indicates that insertion of the CNGA2 S4-S5 linker has decreased the degree of cooperativity in the CNGA1 channels.

In analogy to the analysis of the EC_{50} value, we compared the Hill coefficient in dependence of the presence of one, two, or three additional intracellular CNGA2 regions in a CNGA1 background. The results are (Fig. 3):

1. Together with the CNGA2 CNBD, which also decreased the Hill coefficient when substituted alone, the S4-S5 linker effect remained.
2. The S4-S5 linker effect could be prevented by the additional presence of the CNGA2 C-linker.

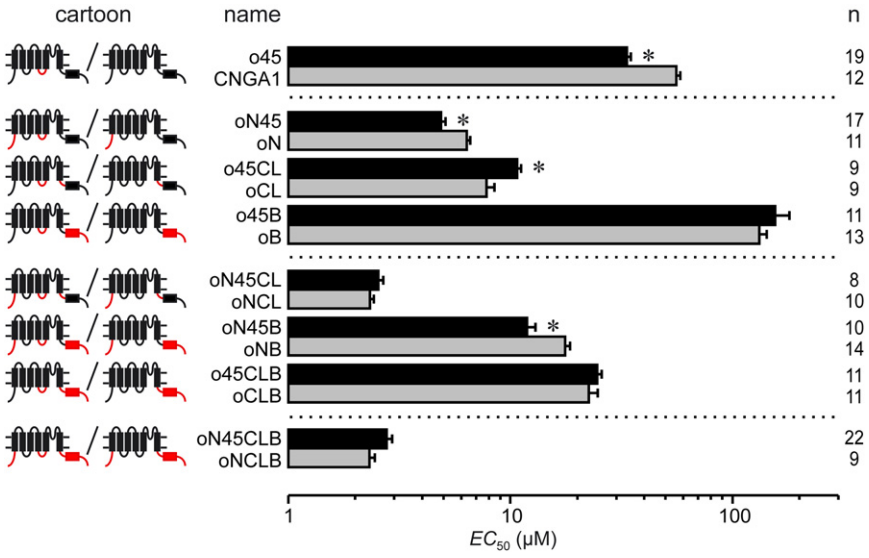

FIGURE 2 Effect of the CNGA2 S4-S5 linker on the cGMP concentration of half-maximum activation, EC_{50}, in a CNGA1 background. The intracellular regions N-terminus, C-linker, and CNBD were systematically substituted. (*Left*) Cartoons and names of the chimeras; (*right*) number of experiments, *n*. In the cartoon: (*red lines* and *boxes*) CNGA2 regions; (*black lines* and *boxes*) CNGA1 regions. (*Asterisks*) Significant difference between the EC_{50} values of the compared chimeras. Statistical data are given as mean ± SE.

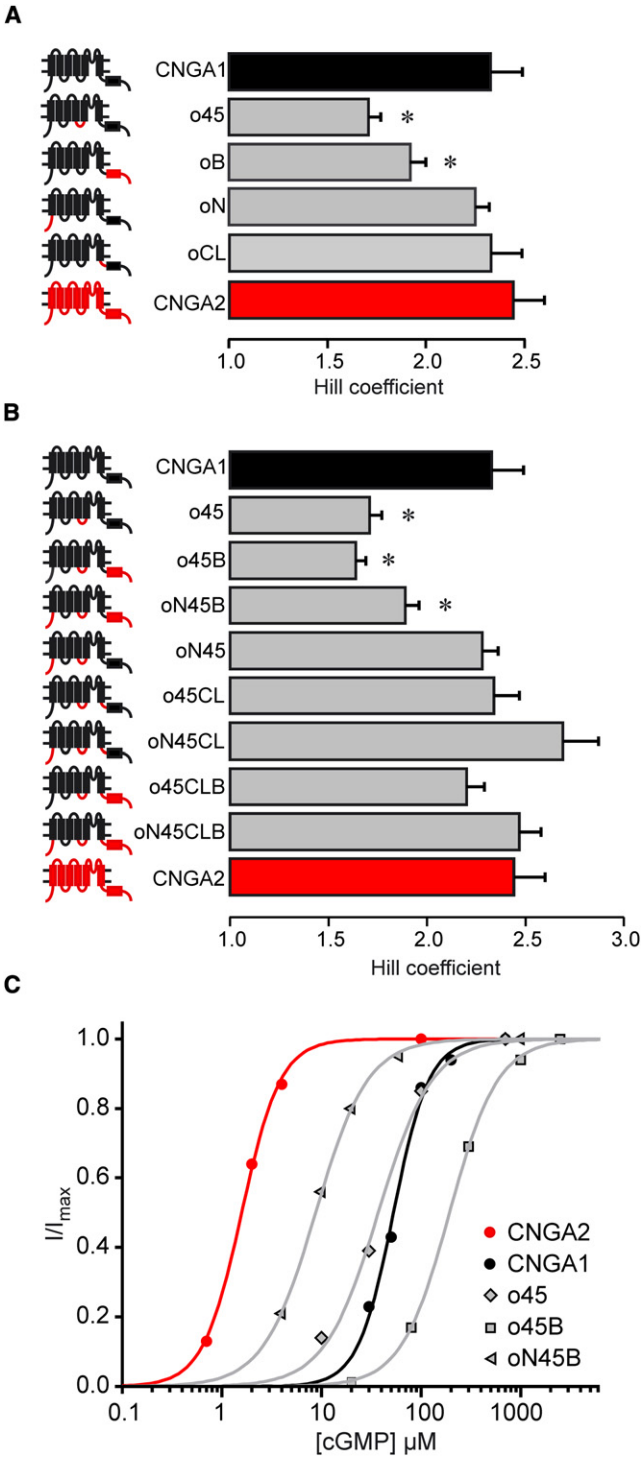

FIGURE 3 Effect of the CNGA2 S4-S5 linker on the Hill coefficient, H, in dependence of the origin of the other intracellular regions N-terminus, C-linker, and CNBD. (*A* and *B*) Hill coefficients of single chimeras, and of all chimeras containing the CNGA2 S4-S5 linker. The values of the two wild-type channels CNGA1 and CNGA2 are given for comparison. (*Left*) Cartoons and names of the chimeras. (*Red lines* and *red boxes*) CNGA2 regions; (*black lines* and *black boxes*) CNGA1 regions. (*Asterisks*) Hill coefficients significantly different from that of CNGA1 channels. Statistical data are given as mean ± SE. (*C*) Representative concentration-response relations of individual patches for the two wild-type channels CNGA1 (*black circles* and *black line*) and CNGA2 (*red circles* and *red line*), and of the chimeras with a significantly decreased Hill coefficient (*gray symbols* and *gray lines*) after substitution of the S4-S5 linker. (*Lines*) Best fits with the Hill equation (see Eq. 1).

3. The S4-S5 linker effect could be prevented by the additional presence of the CNGA2 N-terminus, but only if the CNGA2 CNBD was not also transferred.

The latter effect is most likely due to the fact, that the own decreasing effect of the CNBD can not be prevented by the N-terminus (oNB: $H = 1.93 \pm 0.11$ (not shown); oB: $H = 1.92 \pm 0.08$).

The N-terminus and the C-linker had no effect on the Hill coefficient, when substituted alone or together (oN: $H = 2.24 \pm 0.07$; oCL: $H = 2.32 \pm 0.15$ (Fig. 3 *A*); oNCL: $H = 2.22 \pm 0.12$ (not shown)).

Interaction energies of intracellular CNGA2 regions associated with activation gating

To decide whether the effects of two intracellular regions on channel gating are coupled, we calculated the differences of the standard molar Gibbs free energy, $\Delta_r G^{\oplus}$ (Eq. 6), and the interaction energies, $\Delta_{int} G^{\oplus}$ (Eq. 7), following the principles of thermodynamic double-mutant cycle analysis (see Materials and Methods; for review, see (38–40)). If the effects of the two substituted regions are coupled, the interaction energy differs from zero. Differences of interaction energies equaling zero indicate that either there is no interaction between the regions (i.e., the effects of a substitution are solely additive) or that the interaction between the two substituted regions is of the same magnitude as the interaction of the two respective wild-type regions.

Considering the interaction of the S4-S5 linker with the N-terminus, we found a negative interaction energy in an otherwise unchanged CNGA1 background, as well as in the presence of the CNGA2 C-linker and in the presence of the CNGA2 CNBD (Fig. 4). In analogy, we found a negative interaction energy for the pair of S4-S5 linker and C-linker in an otherwise unchanged CNGA1 background, as well as in the presence of the CNGA2 N-terminus and in the presence of the CNGA2 CNBD. In contrast, the interaction energies for the pair of S4-S5 linker and CNBD were, in none of the cases tested, significantly different from zero.

Finally, all interaction energies between the S4-S5 linker and one of the other intracellular regions were calculated in the presence of the two remaining CNGA2 regions. None of the possible combinations resulted in significant interaction energies (data not shown). This shows that if two CNGA2 regions are inserted in a CNGA1 background, the gating is already determined by them and cannot be further modulated by the respective other intracellular CNGA2 regions transferred additionally.

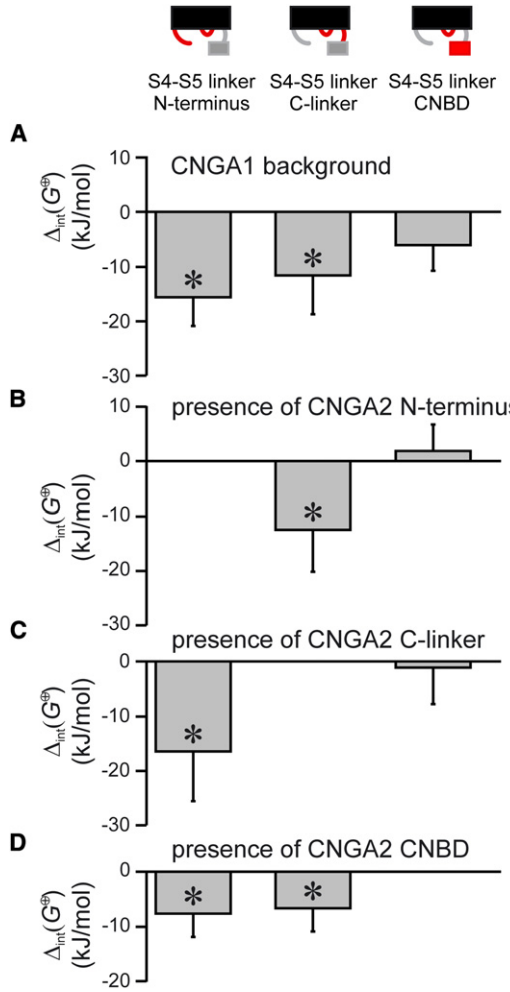

FIGURE 4 Interaction energies, $\Delta_{int}G^{\oplus}$, between the CNGA2 S4-S5 linker and one of the other intracellular CNGA2 regions tested, in an otherwise unchanged CNGA1 background and in the presence of one other CNGA2 region. Cartoons in the upper part illustrate the two CNGA2 regions whose interaction energy is calculated. (*Red lines* and *boxes*) CNGA2 regions; (*gray lines* and *gray boxes*) CNGA1 or CNGA2 regions; (*black boxes*) transmembranal CNGA1 background. (*A*) $\Delta_{int}G^{\oplus}$ in an otherwise unchanged CNGA1 background. (*B–D*) $\Delta_{int}G^{\oplus}$ in the presence of the indicated CNGA2 region. Asterisks assign interaction energies differing significantly from zero. Statistical data are given as mean ± SE.

DISCUSSION

Our results show that the S4-S5 linker codetermines the activation gating of CNG channels together with the other intracellular regions N-terminus, C-linker, and CNBD and that there are specific interactions among these regions.

Substitution of the N-terminus or the C-linker in an otherwise unchanged CNGA1 background by the respective region from CNGA2 causes a shift of the concentration-response relationship to lower cGMP concentrations, i.e., the apparent affinity for cGMP increases and the chimera is more similar to the donor channel CNGA2 than the acceptor channel CNGA1 (oN and oCL in Fig. 2). These data confirm previous results showing that the N-terminus (13,19,20) and the C-linker (12–15,17,18,20) are determinants of the characteristic EC_{50} value in CNG channels. To our surprise, also substitution of the S4-S5 linker (o45) caused a noticeable shift of the concentration-response relationship to smaller cGMP concentrations. In contrast to the N-terminus, the C-linker, and the S4-S5 linker, substitution of the CNBD (oB) paradoxically decreased the apparent affinity to cGMP, as shown previously (compare to (20)).

While the effect of the CNGA2 N-terminus, the C-linker, and the CNBD did not depend on the nature of the other intracellular regions (data not shown), the effect of the S4-S5 linker did (Fig. 2): In double chimeras, the N-terminus did not hinder the S4-S5 linker effect, the C-linker inverted it, and the CNBD neutralized it. In the presence of CNGA2 N-terminus plus C-linker there was no further S4-S5 linker effect, possibly due to the opposite effects of these two additional regions, as observed in the double chimeras. The modulatory effect of the CNGA2 C-linker, but not that of the CNGA2 N-terminus, on the CNGA2 S4-S5 linker, could be abolished by the CNGA2 CNBD. This susceptibility of the S4-S5 linker to the origin of the surrounding intracellular regions indicates an interaction of the S4-S5 linker with these regions, either in a direct or indirect way (see below). Together, our results regarding the EC_{50} values show that the apparent affinity of a channel to a ligand is not predominantly controlled by the CNBD, but by multiple interactions of at least three different regions within the intracellular channel portion, including the S4-S5 linker.

In addition to the effects on the apparent affinity, each of the four regions influenced the Hill coefficient (Fig. 3). It was decreased by the CNGA2 S4-S5 linker and CNBD alone, suggesting a direct disturbing effect of these CNGA2 regions on the cooperativity of the subunits, when operating in a CNGA1 background. The N-terminus and the C-linker had no such effect when substituted alone, suggesting either that these two regions are not important for the cooperativity of the four subunits, or that the CNGA2 regions in a CNGA1 background mimic the effect of the respective natural CNGA1 region.

The latter question can be further addressed by considering the double, triple, and quadruple chimeras: Because the CNGA2 C-linker prevented the disturbing effect of the S4-S5 linker when substituted together, the C-linker also influences the cooperativity between the subunits. This preventing effect could be observed in all chimeras containing the CNGA2 C-linker and S4-S5 linker. In addition, the CNGA2 N-terminus prevented the disturbing effect of the S4-S5 linker when substituted together. Hence, the N-terminus is also involved in controlling the cooperativity of the subunit action. It is notable that the CNGA2 N-terminus was ineffective to prevent the disturbing effect of the CNGA2 S4-S5 linker when, in addition, the CNGA2 CNBD was substituted. This suggests that the disturbing effect of the CNGA2 CNBD cannot be cancelled by

the CNGA2 N-terminus. It is notable that our result of a crucial role of the S4-S5 linker for the cooperativity in CNG channels corresponds to previous results in related HERG (42) and *Shaker* channels (28).

Structurally, the S4-S5 linkers of CNGA1 and CNGA2 are both only 11 amino acids long and they differ by only a single residue (11,26). Hence, the linker substitution is in fact the substitution of an asparagine at position 291 in CNGA1 by a serine. The N-terminal part of the S4-S5 linker is predominantly hydrophilic and the C-terminal part predominantly hydrophobic, separated by the structure-breaking amino-acid proline in the middle. Based on the amino-acid sequence (11,26) it is not likely that the S4-S5 linker forms an α-helix, as reported for voltage-gated *Shaker* and HCN channels (27–29). Therefore, to us, the identified influence of the S4-S5 linker on the CNG channel activation was unexpected.

To quantify the interaction intensity between two intracellular regions, interaction energies $\Delta_{int}G^{\oplus}$ were considered, thereby assuming that the principles of thermodynamic double-mutant cycle analysis developed for the interaction of mutated amino acids (38–40) also hold for the interaction of whole intracellular regions (41,43).

To begin, the interaction of the S4-S5 linker with the C-linker is considered (Fig. 4, *A–D*, *middle columns*). Independent of the nature of the other intracellular regions, the combined substitution of these two regions resulted consistently in negative interaction energies. An interaction between the S4-S5 linker and the C-linker seems to be plausible when considering structural data of voltage-gated potassium channels (44) and the C-terminal part of related HCN channels (23), which both suggest a close proximity of these regions. In addition to this, it has been reported that in HCN channels these two regions functionally interact (45–47).

Negative interaction energies were also consistently observed for the interaction of the S4-S5 linker and the N-terminus with all other combinations of intracellular regions (Fig. 4, *A–D*, *left columns*). In contrast to the interaction between the S4-S5 linker with the C-linker, this interaction could, a priori, not be expected because reliable structural data are not available. We propose that the N-terminus adopts a structure of which at least a part is in close proximity to the S4-S5 linker. This idea bears analogy to an interaction between the N-terminus and the S4-S5 linker upon N-type inactivation in *Shaker* channels. Here the S4-S5 linker works as a receptor for the N-terminus (27). An extensive interaction between these regions has also been proposed for the activation of eag and HERG channels (48–50).

In contrast to the interaction of the S4-S5 linker with the N-terminus and the C-linker, our analysis did not yield $\Delta_{int}G^{\oplus}$ values significantly different from zero for the interaction of the CNGA2 S4-S5 linker with the CNGA2 CNBD. This negative result suggests either that the interaction of the respective native CNGA1 regions is similar to the CNGA2 regions or that there is no interaction between these regions at all. Assuming that the S4-S5 linker resides closely to the transmembranal part of the channel and that the C-linker forms a compact structure between the transmembranal part and the CNBD, thereby separating both regions from each other (23), it is somehow intuitive that these two regions do not interact.

For related tetrameric voltage-gated channels, such as Kv and HCN channels, there is strong evidence that the S4-S5 linker plays an important role in transferring the movement of the voltage sensing S4-helix to the pore-forming helices S5 and S6 (51,45), thereby controlling the channel gate. In these channels, the S4-S5 linker is an α-helix with the ability to mechanically couple these two regions. In contrast, the S4-S5 linker of CNG channels does not form an α-helix, but rather, a loop with a conserved proline in the middle, which is assumed to reduce the mechanical coupling between the S4-helix and the pore-forming helices S5 and S6 (30).

Thus, one can speculate that the communication pathway between these two channel parts is very loose, and thus ineffective. In the light of this, it was even more surprising to observe that the S4-S5 linker does influence both the apparent affinity to cGMP and the cooperativity between the subunits. When also taking into account our results of an interaction between the S4-S5 linker with the N-terminus and the C-linker, our data suggest that this influence is mediated via the N-terminus and the C-linker, whereas a direct interaction between the S4-S5 linker and the CNBD seems to be unlikely. Hence, our systematic exchange of a second, third, and fourth intracellular region, together with the S4-S5 linker, provides the result that there is an intensive interaction among all four intracellular regions during the activation process, including the S4-S5 linker.

It is finally notable that in no case did the insertion of two intracellular CNGA2 regions in the presence of the two other CNGA2 regions result in energy values differing significantly from zero (data not shown). With respect to the conclusions mentioned above, this result suggests that substitution of three CNGA2 regions exerts already the maximum effect on channel activation, independent of which of the three CNGA2 regions are combined. Apparently, there is some functional redundancy among the four intracellular CNGA2 regions to activate the channels.

We are indebted to U.B. Kaupp (Caesar, Bonn, Germany) for providing the wild-type and five of the chimeric clones. We are also grateful to Karin Schoknecht, S. Bernhardt, A. Kolchmeier, G. Sammler, and B. Tietsch for excellent technical assistance.

This work was supported by the grants BE 1250/14-4 and BE 1250/16-1 of the Deutsche Forschungsgemeinschaft to K.B.

REFERENCES

1. Kaupp, U. B. 1991. The cyclic nucleotide-gated channels of vertebrate photoreceptors and olfactory epithelium. *Trends Neurosci.* 14:150–157.

2. Distler, M., M. Biel, …, F. Hofmann. 1994. Expression of cyclic nucleotide-gated cation channels in non-sensory tissues and cells. *Neuropharmacology.* 33:1275–1282.
3. Kaupp, U. B., and R. Seifert. 2002. Cyclic nucleotide-gated ion channels. *Physiol. Rev.* 82:769–824.
4. Zagotta, W. N., and S. A. Siegelbaum. 1996. Structure and function of cyclic nucleotide-gated channels. *Annu. Rev. Neurosci.* 19:235–263.
5. Chen, T. Y., Y. W. Peng, …, K. W. Yau. 1993. A new subunit of the cyclic nucleotide-gated cation channel in retinal rods. *Nature.* 362:764–767.
6. Körschen, H. G., M. Illing, …, R. S. Molday. 1995. A 240 kDa protein represents the complete β subunit of the cyclic nucleotide-gated channel from rod photoreceptor. *Neuron.* 15:627–636.
7. Bönigk, W., J. Bradley, …, S. Frings. 1999. The native rat olfactory cyclic nucleotide-gated channel is composed of three distinct subunits. *J. Neurosci.* 19:5332–5347.
8. Zheng, J., W. N. Zagotta, and W. N. Zagotta. 2000. Gating rearrangements in cyclic nucleotide-gated channels revealed by patch-clamp fluorometry. *Neuron.* 28:369–374.
9. Weitz, D., N. Ficek, …, U. B. Kaupp. 2002. Subunit stoichiometry of the CNG channel of rod photoreceptors. *Neuron.* 36:881–889.
10. Zhong, H., L. L. Molday, …, K. W. Yau. 2002. The heteromeric cyclic nucleotide-gated channel adopts a 3A:1B stoichiometry. *Nature.* 420:193–198.
11. Kaupp, U. B., T. Niidome, …, S. Numa. 1989. Primary structure and functional expression from complementary DNA of the rod photoreceptor cyclic GMP-gated channel. *Nature.* 342:762–766.
12. Gordon, S. E., and W. N. Zagotta. 1995. Localization of regions affecting an allosteric transition in cyclic nucleotide-activated channels. *Neuron.* 14:857–864.
13. Gordon, S. E., and W. N. Zagotta. 1995. A histidine residue associated with the gate of the cyclic nucleotide-activated channels in rod photoreceptors. *Neuron.* 14:177–183.
14. Zong, X., H. Zucker, …, M. Biel. 1998. Three amino acids in the C-linker are major determinants of gating in cyclic nucleotide-gated channels. *EMBO J.* 17:353–362.
15. Paoletti, P., E. C. Young, and S. A. Siegelbaum. 1999. C-Linker of cyclic nucleotide-gated channels controls coupling of ligand binding to channel gating. *J. Gen. Physiol.* 113:17–34.
16. Johnson, Jr., J. P., and W. N. Zagotta. 2001. Rotational movement during cyclic nucleotide-gated channel opening. *Nature.* 412:917–921.
17. Broillet, M. C., and S. Firestein. 1996. Direct activation of the olfactory cyclic nucleotide-gated channel through modification of sulfhydryl groups by NO compounds. *Neuron.* 16:377–385.
18. Gordon, S. E., M. D. Varnum, and W. N. Zagotta. 1997. Direct interaction between amino- and carboxyl-terminal domains of cyclic nucleotide-gated channels. *Neuron.* 19:431–441.
19. Goulding, E. H., G. R. Tibbs, and S. A. Siegelbaum. 1994. Molecular mechanism of cyclic-nucleotide-gated channel activation. *Nature.* 372:369–374.
20. Möttig, H., J. Kusch, …, K. Benndorf. 2001. Molecular regions controlling the activity of CNG channels. *J. Gen. Physiol.* 118: 183–192.
21. Varnum, M. D., and W. N. Zagotta. 1997. Interdomain interactions underlying activation of cyclic nucleotide-gated channels. *Science.* 278:110–113.
22. Rosenbaum, T., and S. E. Gordon. 2002. Dissecting intersubunit contacts in cyclic nucleotide-gated ion channels. *Neuron.* 33:703–713.
23. Zagotta, W. N., N. B. Olivier, …, E. Gouaux. 2003. Structural basis for modulation and agonist specificity of HCN pacemaker channels. *Nature.* 425:200–205.
24. Craven, K. B., and W. N. Zagotta. 2004. Salt bridges and gating in the COOH-terminal region of HCN2 and CNGA1 channels. *J. Gen. Physiol.* 124:663–677.
25. Hua, L., and S. E. Gordon. 2005. Functional interactions between A′ helices in the C-linker of open CNG channels. *J. Gen. Physiol.* 125:335–344.
26. Ludwig, J., T. Margalit, …, U. B. Kaupp. 1990. Primary structure of cAMP-gated channel from bovine olfactory epithelium. *FEBS Lett.* 270:24–29.
27. Isacoff, E. Y., Y. N. Jan, and L. Y. Jan. 1991. Putative receptor for the cytoplasmic inactivation gate in the *Shaker* K^+ channel. *Nature.* 353:86–90.
28. Holmgren, M., M. E. Jurman, and G. Yellen. 1996. N-type inactivation and the S4-S5 region of the *Shaker* K^+ channel. *J. Gen. Physiol.* 108:195–206.
29. Ohlenschläger, O., H. Hojo, …, P. I. Haris. 2002. Three-dimensional structure of the S4-S5 segment of the *Shaker* potassium channel. *Biophys. J.* 82:2995–3002.
30. Anselmi, C., P. Carloni, and V. Torre. 2007. Origin of functional diversity among tetrameric voltage-gated channels. *Proteins.* 66:136–146.
31. Rosenbaum, T., A. Gordon-Shaag, …, S. E. Gordon. 2004. State-dependent block of CNG channels by dequalinium. *J. Gen. Physiol.* 123:295–304.
32. Nache, V., E. Schulz, …, K. Benndorf. 2005. Activation of olfactory-type cyclic nucleotide-gated channels is highly cooperative. *J. Physiol.* 569:91–102.
33. Biskup, C., J. Kusch, …, K. Benndorf. 2007. Relating ligand binding to activation gating in CNGA2 channels. *Nature.* 446:440–443.
34. Colquhoun, D. 1998. Binding, gating, affinity and efficacy: the interpretation of structure-activity relationships for agonists and of the effects of mutating receptors. *Br. J. Pharmacol.* 125:924–947.
35. Li, J., W. N. Zagotta, and H. A. Lester. 1997. Cyclic nucleotide-gated channels: structural basis of ligand efficacy and allosteric modulation. *Q. Rev. Biophys.* 30:177–193.
36. Weiss, J. N. 1997. The Hill equation revisited: uses and misuses. *FASEB J.* 11:835–841.
37. Hamill, O. P., A. Marty, …, F. J. Sigworth. 1981. Improved patch-clamp techniques for high-resolution current recording from cells and cell-free membrane patches. *Pflugers Arch.* 391:85–100.
38. Wells, J. A. 1990. Additivity of mutational effects in proteins. *Biochemistry.* 29:8509–8517.
39. Mildvan, A. S., D. J. Weber, and A. Kuliopulos. 1992. Quantitative interpretations of double mutations of enzymes. *Arch. Biochem. Biophys.* 294:327–340.
40. Horovitz, A. 1996. Double-mutant cycles: a powerful tool for analyzing protein structure and function. *Fold. Des.* 1:R121–R126.
41. Scholle, A., T. Zimmer, …, K. Benndorf. 2004. Effects of Kv1.2 intracellular regions on activation of Kv2.1 channels. *Biophys. J.* 87: 873–882.
42. Sanguinetti, M. C., and Q. P. Xu. 1999. Mutations of the S4-S5 linker alter activation properties of HERG potassium channels expressed in *Xenopus* oocytes. *J. Physiol.* 514:667–675.
43. Sunderman, E. R., and W. N. Zagotta. 1999. Sequence of events underlying the allosteric transition of rod cyclic nucleotide-gated channels. *J. Gen. Physiol.* 113:621–640.
44. Jiang, Y., A. Lee, …, R. MacKinnon. 2003. X-ray structure of a voltage-dependent K^+ channel. *Nature.* 423:33–41.
45. Chen, J., J. S. Mitcheson, …, M. C. Sanguinetti. 2001. The S4-S5 linker couples voltage sensing and activation of pacemaker channels. *Proc. Natl. Acad. Sci. USA.* 98:11277–11282.
46. Decher, N., J. Chen, and M. C. Sanguinetti. 2004. Voltage-dependent gating of hyperpolarization-activated, cyclic nucleotide-gated pacemaker channels: molecular coupling between the S4-S5 and C-linkers. *J. Biol. Chem.* 279:13859–13865.
47. Prole, D. L., and G. Yellen. 2006. Reversal of HCN channel voltage dependence via bridging of the S4-S5 linker and Post-S6. *J. Gen. Physiol.* 128:273–282.

48. Terlau, H., S. H. Heinemann, …, J. Ludwig. 1997. Amino terminal-dependent gating of the potassium channel rat EAG is compensated by a mutation in the S4 segment. *J. Physiol.* 502:537–543.

49. Wang, J., M. C. Trudeau, …, G. A. Robertson. 1998. Regulation of deactivation by an amino terminal domain in human Ether-à-Go-Go-related gene potassium channels. *J. Gen. Physiol.* 112: 637–647.

50. Chen, J., A. Zou, …, M. C. Sanguinetti. 1999. Long QT syndrome-associated mutations in the Per-Arnt-Sim (PAS) domain of HERG potassium channels accelerate channel deactivation. *J. Biol. Chem.* 274:10113–10118.

51. Nishizawa, M., and K. Nishizawa. 2009. Coupling of S4 helix translocation and S6 gating analyzed by molecular-dynamics simulations of mutated Kv channels. *Biophys. J.* 97:90–100.